Designing Lithium-sulfur Batteries with High-loading Cathodes at a Lean Electrolyte condition

*Sheng-Heng Chung and Arumugam Manthiram**

AUTHOR ADDRESS

Dr. S.-H. Chung, Prof. A. Manthiram

Materials Science and Engineering Program & Texas Materials Institute

The University of Texas at Austin, Austin, TX 78712, USA

*E-mail: manth@austin.utexas.edu (A. Manthiram)

KEYWORDS

lithium-sulfur batteries, high sulfur loading, high sulfur content, low electrolyte amount, cycle life

ABSTRACT

Developing lithium-sulfur cells with a high-loading cathode at a lean-electrolyte condition is the key to bringing the lithium-sulfur technology into the energy-storage market. However, it has proven extremely challenging to develop a cell that simultaneously satisfies the above-mentioned metrics while also displaying high electrochemical efficiency and stability. Here, we present a concept of constructing a conductive cathode substrate with a low surface area and optimized nanoporosity (*i.e.*, limited micropores in the porous matrix) that enables achieving a high sulfur loading of 13 mg cm^{-2} and a high sulfur content of 75 wt.% with an extremely low electrolyte/sulfur ratio of just 4.0 μL mg^{-1}. The high-loading nanocomposite cathodes demonstrate high areal capacities of 9.3 mAh cm^{-2}, high energy densities of 18.6 mWh cm^{-2}, and superior cyclability with excellent capacity retention of 85% after 200 cycles. These values are higher than the benchmarks set up for developing future commercial lithium-sulfur cells (*i.e.*, areal capacity of > 2 – 4 mAh cm^{-2}, energy density of > 8 – 13 mWh cm^{-2}, and a long cycle life of 200 cycles with a capacity retention of 80%). The cathode design further exhibits high rate capability from C/20 to 1C rates and great potential to attain ultrahigh sulfur loading and content of 17 mg cm^{-2} and 80 wt.%. The key nanostructural feature that enables realizing fast charge-transport is the low surface area and limited microporosity that avoid the fast consumption of the electrolyte during cell cycling.

With an ever-increasing demand for energy, the society now requires rechargeable batteries with high energy density at an affordable manufacturing and operational costs. Lithium-sulfur batteries, with a high-capacity sulfur cathode (theoretical capacity: 1,675 mAh g^{-1})[1-3] that utilize a two-electron electrochemical conversion reaction, meet these needs due to the high energy density of ~ 2,600 mWh g^{-1} and use of comparatively low-cost active materials.[2,4] However, the lithium-sulfur technology is plagued by serious roadblocks, including the inability to host enough active material to reach a sufficient sulfur loading of 7 – 10 mg cm^{-2} [3,5-7] and a necessary sulfur content of 60 – 80 wt.%,[6-8] while reducing the electrolyte consumption to an acceptable low electrolyte/sulfur ratio of < 5 μL mg^{-1}.[7,9,10] Currently, although much progress has been made in each individual parameter, a comprehensive optimization of all the above parameters has rarely been reported, as commented in the many research and review articles.[3,7,9,11] Moreover, a cell operating under the above strict conditions is now required to attain an effective capacity of over 2 – 4 mAh cm^{-2} and a competitive energy density of 8 – 13 mWh cm^{-2} for commercialization of the Li-S technology.[5-13] On the other hand, the cyclability for making the Li-S technology commercially viable is set at a high capacity retention of 80% after 200 cycles at a high current rate of C/10 during charge- discharge.[3,13,14] However, this task, even in just making the cell normally cycling, has proven extremely difficult.[11,15,16]

According to the conversion-reaction electrochemistry of sulfur cathodes, extrinsic cell-design parameters, such as the amount of sulfur and electrolyte added into the cell, largely dominate the performance and lifetime of lithium-sulfur cells.[3-10,11] The first problem impacting the cell electrochemistry is the insulating nature of sulfur (~10^{-30} S cm^{-1}) and its end-discharge product Li_2S (~10^{-14} S cm^{-1}),[3-5] which causes high cathode resistance that increases the cell polarization and thus decreases the reaction kinetics, hampering the development of high-loading

sulfur cathodes[17,18] and impairing the electrochemical efficiency and reversibility of high-loading sulfur cathodes.[3,17,18]

Further issues originate during cell cycling. The repeated dissolution of the active material and its subsequent deposition on the cathode are coupled with the generation of a series of soluble polysulfides (Li_2S_{4-8})[1-4,9] and a large volume change of 80% between sulfur (2.07 g cm^{-3}) and Li_2S (1.66 g cm^{-3}).[1,4,13] Without a suitable cathode and/or cell architecture, the polysulfides readily dissolve in the electrolyte and gradually change the electrolyte's viscosity, conductivity, and composition.[4,19-21] The uncontrolled physicochemical deterioration of the electrolyte makes it difficult to design a cell that maintains a lean electrolyte condition (*i.e.*, an electrolyte/sulfur ratio of less than 5 μL mg^{-1}).[3,10,19] One yet more difficult task is to maintain fast lithium-ion transport in a lean-electrolyte cell (due to the rapidly increasing viscosity as the electrolyte deteriorates),[5-7,19] which affects the electrochemical reversibility and rate performance during long-term cycling.[7,19-21]

The challenges of lithium-sulfur batteries, however, are not solely limited to the electrolyte. Dissolved polysulfides that either irreversibly diffuse out of the cathode or relocate between the two electrodes is also a significant issue that results in rapidly declining capacity and low Coulombic efficiency.[4,19] Cathodes possessing either a sufficient sulfur loading of > 7 – 10 mg cm^{-2} or sulfur content of over 60 – 80 wt.% magnify the amount and concentration of soluble polysulfides produced, resulting in an even more severe polysulfide diffusion that accelerates the capacity drop within just 50 – 100 cycles.[3,5,13] Additionally, inside the cathode, volume changes occurring during cycling damage the integrity of the high-loading sulfur cathodes, isolating the high amount of insulating sulfur from the conductive agents and the

aluminum-foil current collector.[3,17,18] These problems require a high-loading cathode engineered with high mechanical strength without unduly increasing the cost of the cathode design.[3,6,13,17]

Although various strategies have been exploited to optimize the cathode architecture (*e.g.*, porous current collectors,[22] three-dimensional electrode substrates,[23] and interlayers between the cathode and the separator[24])[1-3,11] and/or components (e.g., nanocomposite cathodes,[1-3,12] polysulfide catholytes,[25,26] and electrolytes[9,10]),[2,5,11,16] major advances reported in the literature have been confined to the achievement of one or two of these aforementioned design metrics (*e.g.*, sulfur loading, sulfur content, electrolyte/sulfur ratio, and cell performance).[27-31] Synchronous improvements in all of the necessary parameters simultaneously have not yet been realized to comprehensively optimize the amounts of sulfur and electrolyte while simultaneously maintaining acceptable electrochemical performance (*i.e.*, high electrochemical cyclability, efficiency, and cell life) due to the complexity of lithium-sulfur chemistry.[3,5,26-28]

The complex lithium-sulfur chemistry includes the use of electronically and ionically insulating sulfur active material to generate a high charge-storage capacity, which limits the reaction kinetics,[3-5] making it essential to generate electrochemically active, soluble polysulfides to achieve high electrochemical utilization and rate capability. However, the electrochemical efficiency and stability fade once the polysulfides begin their irreversible relocation in the cell during cycling.[19,26] In most cases, a large amount of conductive carbon is mixed with sulfur to realize the necessary electrical conductivity for the cell operation.[2,5-8] High porosity is further required for the conductive carbon to accumulate the polysulfides and accommodate the volume changes of the encapsulated active material.[1-5] However, the high amount of carbon added makes it difficult to realize the high-energy-density advantages of sulfur cathode that requires a high sulfur loading and content simultaneously within a cathode.[3,5,26] The overuse of porous carbon

also requires ample amount of electrolyte to maintain a good electron/ion-transfer interface with the active material.[6,7,9] Thus, having either an insufficient amount of sulfur or a high amount of electrolyte can cause the overall cell performance to be unrealistically overestimated and hurt the practical feasibility.[3-7,29] Keeping both of these critical parameters outside the practically necessary regimes further obstructs our ability to understand the true potential and challenges of lithium-sulfur technology.[3-7]

Herein, we present a three-dimensional carbon-paper cathode that incorporates both high sulfur loadings (13 and 17 mg cm^{-2}) and contents (75 and 80 wt.%). This composite cathode possesses a self-assembled current-collector-free design, which excludes the use of extra binders and aluminum-metal current collector. Thus, such a high sulfur loading and content of 13 mg cm^{-2} and 75 wt.% in the current-collector-free cathode realizes a high gravimetric capacity of 535 mAh g^{-1}, high areal capacity of 9.3 mAh cm^{-2}, and high areal energy density of 18.6 mWh cm^{-2} at a low electrolyte/sulfur ratio of 4.0 μL mg^{-1}. The corresponding values at 17 mg cm^{-2} and 80 wt.% sulfur are 473 mAh g^{-1}, 10.2 mAh cm^{-2}, and 19.5 mWh cm^{-2}. As a reference, the gravimetric capacity is calculated based on the total cathode mass including the carbon paper. These high-loading cathodes also demonstrate superior long-term cycle stability, exhibiting a long cycle life of 200 cycles and high capacity retention of 85%. These cell performances outperform the benchmarks established for the development of a viable commercial rechargeable battery, including an areal capacity of over 2 – 4 mAh cm^{-2} and an areal energy density of 8 – 13 mWh cm^{-2} as well as a long cycle life of 200 cycles. In addition, through an analysis of the electrochemical impedance spectroscopy (EIS) and cyclic voltammetry (CV) data, we evidence that the conductive cathode substrate with low nanoporosity plays a key role in facilitating high reaction kinetics in the cells and in limiting the fast, continuous consumption of electrolyte

during cycling.[14,32,33] These would be the two necessary materials characteristics for the design of high-performance lithium-sulfur battery cathodes with high effective capacities together with a long cycle life.

RESULTS AND DISCUSSION

Development of high-loading sulfur cathodes with lean electrolyte

In order to test the ability to host a high amount of sulfur and simultaneously reduce the electrolyte/sulfur ratio, we fabricated a three-dimensional cathode architecture by assembling two carbon-paper sheets that possess high conductivity and low nanoporosity (see Figure S1 and Table S1 in the Supporting Information) to overcome the drawbacks of utilizing too much conductive carbon additives and excess electrolyte in a conventional sulfur cathode configuration.[3,5,26-28] We prepared two high-loading sulfur cathodes with different amount of sulfur by adding, respectively, 45 and 60 μL of 1.5 M Li_2S_6 polysulfide catholyte in the cathode substrate. The carbon-paper cathode substrate hosts well the viscous high-concentration polysulfide catholyte and forms a self-assembled current-collector-free design, which excludes the use of extra binders and aluminum-metal current collector. The resulting two cathodes have large sulfur loadings of 13 or 17 mg cm^{-2}, high sulfur contents of 75 or 80 wt.%, and lean electrolyte/ratios of 4.0 or 3.9 μL mg^{-1} (see Figure S2 in the Supporting Information).

Figures 1a-e and Figures 1f-j show the scanning electron microscopy (SEM) images and energy dispersive x-ray spectroscopy (EDS) results of the cathode, respectively, before and after cycling for 200 cycles. The EDS spectra are summarized in Figure S3 (Supporting Information). In the cross-sectional SEM/EDS (Figures 1a and 1b), the freshly-made cathode shows weak sulfur signals detected from the outside surfaces of the two carbon paper sheets and strong

signals within and on the inside surfaces. The aerial-view SEM/EDS of the outside surfaces of the two carbon paper sheets (Figures 1c and 1e) confirms this by displaying an open porous network, without any signs of obvious polysulfide catholyte filling, and weak elemental sulfur signals. In contrast to the outside surfaces, Figure 1d shows the inside surface of the carbon paper that is filled with and uniformly coated by polysulfides, which is reflected in the strong elemental sulfur signals in the EDS mapping results. The equal distribution and infiltration of the active material is due to the high mobility of the catholyte,[19,23,26] which improves the fabrication of high-loading cathodes.[14,23,26]

After cycling, the three-dimensional carbon-paper cathode expanded in thickness by ~ 50% (from 140 to 210 μm). The expansion of the carbon-paper cathode after cycling is possibly due to the phase transition between the liquid-state polysulfide catholyte and the solid-sate sulfur and sulfides, as well as the volume change between sulfur and lithium sulfide. Moreover, the use of a high amount of sulfur in the carbon-paper cathode amplifies the levels of volume changes during repeated cycling. Thus, after tolerating the huge volume changes brought about by different sulfur species, the carbon-paper cathode might become relatively loose. However, the cycled cathodes retrieved from the cells show neither obvious damages nor broken areas (see Figure S4 in the Supporting Information). The high integrity of the cycled cathode indicates that the three-dimensional cathode architecture possesses good tolerance toward volume changes of the high amount of encapsulated sulfur.[2,23] Moreover, the cycled cathodes continue to display weak elemental sulfur intensity on the outside surfaces, as shown in the cross-sectional SEM/EDS results (Figures 1f and 1g), confirming neither severe polysulfide diffusion nor active-material loss from the cathode. The aerial-view SEM/EDS (Figures 1h-j) affirms this statement and also indicates good sulfur encapsulation throughout the inside region of the carbon-paper

cathode (Figure 1i). The good encapsulation of the catholyte within the three-dimensional carbon-paper electrode architecture guarantees an efficient conductive interface between the conductive cathode substrate and the polysulfide catholyte,[23,29,34] with potentially the good tortuosity of the cathode architecture preventing the uncontrolled diffusion of polysulfides out of the electrode.[2,14,29] These features promote the superior tolerance of a high amount of active material in the cathode[1-3,7] and its volume changes during repeated cycling,[4,5,16] helping us to achieve both high sulfur loading and content while also reducing the electrolyte/sulfur ratio.[3,5-8,35]

Performance of the high-loading sulfur cathodes with lean electrolyte

Figure 2 summarizes the cycling performances and voltage profiles of the cells fabricated with the high-loading sulfur cathodes with a lean electrolyte at C/10, C/7, and C/5 rates. With a sulfur loading and content of 13 mg cm^{-2} and 75 wt.% and an electrolyte/sulfur ratio of 4.0 μL mg^{-1}, the cell was able to deliver peak capacities of 717, 651, and 597 mAh g^{-1} at, respectively, C/10, C/7, and C/5 rates (Figure 2a). After 100 cycles, they retained high reversible capacities of 713, 601, and 563 mAh g^{-1}. All cells achieved a high capacity retention of over 92% and Coulombic efficiency of 98 – 98.9%. Figure 2b demonstrates the cell performance based on the cathode fabricated with a higher sulfur loading of 17 mg cm^{-2} and a sulfur content of 80 wt.% to demonstrate the potential in encapsulating an even higher amount of sulfur in the cathode.[3,5,23] With increasing sulfur loading/content and a lower electrolyte/sulfur ratio of 3.9 μL mg^{-1}, the peak capacities of the cathode remained high at 593, 483, and 360 mAh g^{-1}, with high capacity-retention rates of 92%, 83%, and 80% after 100 cycles at, respectively, C/10, C/7, and C/5 rates. These superior cell performances demonstrate that the three-dimensional carbon-paper cathode

architecture using conductive carbon with low nanoporosity enables the cathode's critical need for a high amount of sulfur with a lean electrolyte for enhanced electrochemical efficiency and stability.[3,5,23,29]

To understand how these high-loading, lean-electrolyte sulfur cathodes are able to cycle so steadily, it is instructive to explore their charge and discharge behaviors as a function of cycle rates and numbers (Figures 2c and 2d). As a result of the high sulfur loading and content as well as the exclusion of using an aluminum-metal current collector, the cathodes that hosted sulfur loadings (contents and electrolyte/sulfur ratios in brackets) of 13 mg cm^{-2} (75 wt.%, 4.0 μL mg^{-1}) and 17 mg cm^{-2} (80 wt.%, 3.9 μL mg^{-1}) were able to attain high gravimetric capacities of, respectively, 535 and 473 mAh g^{-1} at a C/10 rate, as determined by taking into consideration the total mass of the cathode including the carbon papers. Meanwhile, the areal capacities and energy densities of the cathodes approached, respectively, 9.3 – 10.2 mAh cm^{-2} and 18.6 – 19.5 mWh cm^{-2}. These values are almost two times higher than those delivered by commercial $LiCoO_2$ cathodes (4 mAh cm^{-2} and 10.08 mWh cm^{-2}, see Figures S5 and S6 in the Supporting Information), demonstrating the capability of our cathodes to encapsulate a high amount of sulfur and efficiently utilize the hosted active materials at a reasonably high level.[23,26,35] Moreover, the results demonstrate the necessity of fabricating sulfur cathodes, featuring both a high amount of active material and heightened electrochemical characteristics, for realizing a high areal capacity and energy density.[3,5,29]

The voltage profiles of the three-dimensional cathodes hosting different high amounts of sulfur exhibit overlapping discharge and charge curves during 100 continuous cycles at various cycling rates (Figures 2c and 2d). The upper discharge plateaus at ~ 2.3 – 2.0 V correlate to the reduction of sulfur and the formation/migration of polysulfides.[4,19] The overlapping curves

indicate the high polysulfide retention of the cathodes and good electrochemical reversibility of the system.[4,5,19] This behavior then benefits the efficient conversion and stability of the subsequent lower discharge plateaus down to 1.6 V, which involves the liquid-to-solid and solid-to-solid phase transitions.[4,19] The traditional sluggish reaction kinetics of these two steps is mitigated by encapsulating the electrochemically active polysulfides[4,19] in the three-dimensional conductive electrode matrix, which facilitates fast electron transport,[23,26,29] resulting in almost unchanged lower discharge plateaus with a low polarization and average voltage hysteresis of 0.34 and 0.42 V at a C/10 rate for the cathodes having, respectively, 13 and 17 mg cm^{-2} sulfur (see Figures S7 and S8 in the Supporting Information). At a faster C/5 rate, a high current density of up to 4.3 and 5.8 mA cm^{-2} initially causes a high polarization of 0.86 and 0.96 V. The polarization then decreases, demonstrating an active-material rearrangement to a more uniform distribution for high-rate cycling.[3,5,16] This activation cycling at the C/5 rate is commonly found in high-loading cathodes due to the slow reaction kinetics caused by the high sulfur loading[3,26] that is made even worse by the lean electrolyte.[5,26] After that, the three-dimensional carbon-paper cathodes maintain good electrochemical stability, as illustrated with the steady charge and discharge curves.

The high stability brought about by the three-dimensional carbon-paper cathode inspired us to explore the long-term cyclability and reversibility. Figures 3a and 3b display the cathodes with sulfur loadings (contents and electrolyte/sulfur ratios) of 13 mg cm^{-2} (75 wt.%, 4.0 μL mg^{-1}) and 17 mg cm^{-2} (80 wt.%, 3.9 μL mg^{-1}), demonstrating that the electrode is able to achieve high capacity-retention rates of, respectively, 85% and 71% over a long lifetime of 200 cycles. Such a capacity retention satisfies current commercial requirements for the development of lithium-sulfur cells, which need to maintain over 80% of the peak capacity after 200 cycles.[3,14] As we

observed further cycling, the cells eventually became unstable at ~ 250 cycles. However, by replacing the pulverized lithium metal in the counter electrode,[36,37] the cell was able to operate again and reached over 400 cycles with a low capacity-fade rate of 0.045% per cycle (Figure 3c). The capacity recovery demonstrates that our cathodes were not the main source of the cell failure,[13,37] yet it implies another urgent need to develop a stabilized lithium-metal anode for future full-cell testing.[13,36,37]

Investigation of the rate capability and reversibility of the high-loading cathodes

Figure 4a displays the high-rate capability of the three-dimensional carbon-paper cathodes from a slow C/20 to a fast 1C rate. Cathodes with a sulfur loading of 13 mg cm^{-2} and a sulfur content of 75 wt.% delivered a reversible charge-storage capacity approaching 400 mAh g^{-1} with a low electrolyte/sulfur ratio of 4.0 μL mg^{-1} at a high 1C rate. In the voltage profiles (Figure 4b), although the polarization in both the high-loading cathodes (upper part: 13 mg cm^{-2} with a sulfur content of 75 wt.%; lower part: 17 mg cm^{-2} with a sulfur content of 80 wt.%) enlarges as the cycle rate increases from a current density of 1.0 and 1.4 mA cm^{-2} to 21.7 and 28.9 mA cm^{-2}, these high-loading cathodes still attain high capacity-retention rates approaching 90% after the cycling rate is changed back to C/20 after 70 cycles. Such a stable rate capability was demonstrated three times, respectively, from 1–70 cycles, 71–140 cycles, and 141–210 cycles (see Figures S9 – S11 in the Supporting Information).

Although encapsulating electrochemically active polysulfide catholytes within the three-dimensional carbon-paper electrode architecture provides excellent high-rate capability, technical concerns might be raised when transferring this design to pouch cells, which are often used in commercial products.[7,13,14] Therefore, it is imperative to establish a preliminary pouch-

cell prototype to understand whether the three-dimensional carbon-paper electrode architecture possesses enough mechanical strength to be assembled as a larger cathode, as well as whether the electrode architecture can still encapsulate the catholyte within the pouch cell structure. Figures 4c and 4d demonstrate that the three-dimensional carbon-paper cathode implemented in a pouch-cell setup is able to attain a high peak capacity of over 800 mAh g^{-1}. In addition, we made the pouch cell transparent in order to inspect the polysulfide retention during cell assembly and cycling. As shown in Figure S12 (Supporting Information), we pressed the cathode and the assembled pouch cell to observe whether any polysulfide leaked out. During these steps and after operating the device at a C/25 rate for 20 cycles, we observed no obvious polysulfide leakage or cathode damage. The excellent polysulfide retention and cathode mechanical strength proven by this experiment suggest the high potential for further developing our cathode into pouch cells.

Electrochemical impedance and cyclic voltammetry of the high-loading cathodes

The prior analysis affirmed the successful development of the three-dimensional carbon-paper cathode realizing high sulfur loading/content and lean electrolyte. The cells demonstrate outstanding electrochemical efficiency and stability with long life. Considering that the cycle stability and high-rate capability relate to the interfacial charge-transfer process and lithium-ion transfer, we next investigated the electrochemical impedance[29,31,34] and lithium-ion diffusion of the cathodes.[31-33] We used the same high-loading/content sulfur cathode design (13 mg cm^{-2} and 75 wt.%) with a low electrolyte/sulfur ratio of 4.0 μL mg^{-1}. Figure 5 summarizes the analytical result of EIS used to investigate the reaction kinetics.[29,31,34] Figure 5a and Figure S13a (Supporting Information) illustrate the experimental data and the fitting results according to the suggested equivalent-circuit model (see inset).[29,34,38] The low overall cell resistance of 70 – 80

ohms indicates the fast reaction kinetics contributed by the good electrochemical activity of the polysulfide catholyte and the fast electron transport of the carbon-paper substrate.[26,29,33] The fitting results demonstrated in both the Nyquist and Bode plots (Figures 5a and 5b as well as Figures S13a and S13b in the Supporting Information) confirm a high compatibility of the model used, with the real axis referring to the resistance of the electrolyte and the internal ohmic resistance of the cell (R1), the semicircle at high frequency corresponding to the interfacial contact resistance (R2), and the semicircle at the middle frequency caused by the charge-transfer process (R3).[5,29,34,37] Next, we applied the suggested circuit to the impedance results collected with the two different cell-testing techniques to investigate the cell's reaction kinetics as a function of cycle number (Figure 5c) and cycling rates (Figure 5d).

Figure 5c and Figure S13 (Supporting Information) display the EIS analysis as a function of cycle number, which summarizes the experimental and fitting results of the cells every 10 cycles at C/10 rate. The cell shows a slight decrease in the overall impedance from 80 to 60 ohms after cycling, which is mainly associated with the decrease in the interfacial contact resistance caused by the electron transfer through the conductive electrode network to the three-phase boundary involving the active material, electrolyte, and the conductive network within the sulfur cathode.[29,34,38] The overall cell impedance in the subsequent 70 cycles stabilizes at low values of 50 – 60 ohm. The low interfacial contact resistance obtained with the three-dimensional carbon-paper cathode is due to the use of the electrochemically active polysulfide catholyte in the conductive electrode substrate,[26,32,33,38] and its initial decrease is due to the rearrangement of the infiltrated catholyte spread throughout the electrode substrate.[26,38]

Next, we explored the effect of the cycling rate on the electrochemical reaction kinetics. In consideration of the stable cyclability of the three-dimensional carbon-paper cathode for over

200 cycles (Figure 3a) and the stable, low overall and individual impedance values at the C/10 rate (Figure 5c and Figure S13 in the Supporting Information), the impedance data in Figure 5d and Figure S14 (Supporting Information) were collected from one cell with an increasing cycling rate from C/20 to 1C every 10 cycles for the first 70 cycles. The rate was then set back to C/20 at the 71st cycle to analyze the electrochemical reversibility. In the high-loading cell with a lean electrolyte, we found that the interfacial contact resistance was higher than the charge-transfer resistance at a C/20 rate, suggesting that the interfacial contact resistance could dominate the reaction kinetics at low cycling rates. A slow operation rate provides the active material sufficient amount of time to convert into insulating end-discharge products[5,26,38] and from aggregated deposits,[38,39] thus creating low conductive interfaces within the cathode architecture.[4,5,38,39] However, the interfacial contact resistance is reduced at mid-level rates of C/10 and C/7. Then, at high cycling rates of C/5 – 1C, the charge-transfer resistance becomes higher than the interfacial contact resistance so that it dominates the reaction kinetics. This is because the charge-transfer resistance exactly reflects the processes of charge transfer between the conductive electrode network and the active catholyte.[29,38,39] In terms of lithium-sulfur chemistry, a high current density leads to high polarization and incomplete conversion reactions. These problems become stronger when the cells have a high amount of insulting active material that causes high resistance and lean electrolyte that impairs lithium-ion transport.[29,38] We, therefore, hypothesize that the interfacial contact resistance and charge-transfer resistance control the conversion reactions of the sulfur cathode at, respectively, low and high cycling rates. This hypothesis was affirmed by the EIS analytical results for the 71 – 80 and 81 – 90 cycles. When the cycling rates were set back to C/20 again, the slow operation rate provides sufficient amount of time for the charges to transfer completely in the three-dimensional cathode, while the

insulating end-discharge products may form and create low conductive interfaces within the cathode architecture.[38,39] As a result, the interfacial contact resistance again controls the overall impedance and could be the main influence on the reaction kinetics.[29,34] Although the dominant electrochemical units changed from interfacial contact resistance to charge-transfer resistance as the operation rates changed from low to high cycling rates, the overall impedances were low and constant at 60 – 65 ohms.

Since the capability to smoothly transfer charge is necessary for attaining high-rate performance, we studied the lithium-ion diffusion in the high-loading sulfur cathodes with lean electrolyte.[31-33] The lithium-ion diffusion coefficient was calculated by considering the initial CV scans of cells made with high-loading sulfur cathodes (13 mg cm^{-2} and 75 wt.% sulfur) with a low electrolyte/sulfur ratio of 4.0 μL mg^{-1} as a function of the applied scanning rate of 0.02, 0.03, and 0.04 mV s^{-1} (Figure 6a). The CV curves are in agreement with the discharge/charge profiles, demonstrating two cathodic peaks at 2.25 and 2.0 V that correspond to the reduction reaction from solid-state sulfur to soluble polysulfides and the further reduction to solid-state Li_2S_2/Li_2S.[19.29,38] The overlapping anodic peaks at 2.3 and 2.4 V are associated with the coupled oxidation conversions of Li_2S_2/Li_2S to polysulfides and sulfur.[1,4,19] The cathodic and anodic peaks were collected and calculated according to the Randles-Sevcik equation.[31-33]

Figure 6b shows the lithium-ion diffusion coefficients as C1 = 1.2×10^{-7}, C2 = 3.8×10^{-7}, A1 = 1.2×10^{-6}, and A2 = 8.6×10^{-7} cm^2 s^{-1}. C1 and C2 are the cathodic peaks representing the reduction of sulfur to polysulfides and sulfide, respectively, while the overlapping A1 and A2 peaks indicate the anodic peaks for the conversion of sulfides to polysulfides and sulfur, respectively.[1-4,33] Figures S15 and S16 in the Supporting Information show the lithium-ion diffusion coefficients calculated based on the fifth and tenth scans. Figure 6c demonstrates stable

and fast lithium-ion diffusion coefficients, suggesting efficient lithium-ion diffusion in the high-loading sulfur cathode with lean electrolyte.[31,32] The high diffusion coefficient values confirm the high charge-storage capacity per area of the cathodes.[31-33] Figure 6d and Figures S17 and S18 (Supporting Information) display the CV plots at various scanning rates during the initial ten scans. The overlapping curves again affirm the high electrochemical reversibility that is critical for operating a high-loading cathode with lean electrolyte.[5,31]

According to the results summarized in Figures 5 and 6, the interfacial contact resistance and charge-transfer resistance of the high-loading cathode control the major reaction kinetics at, respectively, slow and fast cycling rates.[29,31,34,40] In addition, the steadily fast lithium-ion coefficient is necessary for the sulfur cathode to cycle under a lean electrolyte condition while retaining high capacity output.[31-33,40] These enhanced electrochemical characteristics prove that the conductive, three-dimensional carbon-paper cathode substrate encapsulates a high amount of electrochemically active polysulfide catholyte with high retention, enabling us to realize both low resistance and smooth lithium-ion transport.[5,26,40] Thus, this configuration suggests a potential path forward to construct high-loading cathodes with over 10 mg cm^{-2} sulfur and a high sulfur content of > 75 wt.% to realize high-energy-density lithium-sulfur battery cathodes. In addition, the cathode's limited nanoporosity could simultaneously reduce the consumption of electrolyte during cell assembly and operation.[3,5-10,40]

Progress on the state-of-the-art lithium-sulfur battery cathodes

A growing number of publications in lithium-sulfur technology have witnessed a continuous progress in terms of (1) design conditions, (2) electrochemical performance, and (3) cyclability of lithium-sulfur cells. We herein summarize the research articles that demonstrate a

high-loading sulfur cathode at a lean electrolyte condition, as shown in Figure 7. The detailed cell-design conditions and cell performances were collected and are given in Table S2 (references S1 – S20, Supporting Information) as a reference. In Table S2, most of the research articles that report high-performance sulfur cathodes with a high amount of sulfur at low electrolyte conditions utilize a three-dimensional cathode configuration, including porous carbon films, layered carbon substrates, foam-type current collectors, and core-shell cathodes (Table S2, left first column). On the other hand, the conventional cathode configuration with sulfur/carbon nanocomposites, additional conductive carbons, and binders coated on an alumni-foil current collector faces difficulty in simultaneously attaining a high amount of sulfur, low electrolyte volume, and reasonably high electrochemical performances, especially the cyclability.

Figure 7a shows the sulfur loading and sulfur content values of our cathodes as a comparison with the start-of-the-art high-loading cathodes reported in the literature. The data obtained from our cathodes are marked with red circles. The data collected from references S1 – S20 (Supporting Information) in the supporting information have a sulfur loading of at least 10 mg cm^{-2}. As shown in the plot, our cathode design not only allows high sulfur loadings of up to 13 and 17 mg cm^{-2}, but also achieves the highest sulfur content of as high as 80 wt.% in the cathode. Simultaneously attaining such a high sulfur loading and ultrahigh sulfur content demonstrates the outstanding capability of our cathodes to effectively encapsulate a high amount of sulfur.[9,11]

It is well known in the literature that the amounts of sulfur and electrolyte added in the cathodes would control the effective areal capacity of the cells.[7-9,11] Thus, we next inspect the areal capacity values of our cathodes and the reported high-loading cathodes at an acceptable low electrolyte/sulfur ratio of < 5 μL mg^{-1}.[7,9,10] As shown in Figure 7b, our high-loading cathodes

that host the highest sulfur loading/content are still able to deliver excellent areal capacities higher than the requirements set for commercial rechargeable batteries (an areal capacity of 2 - 4 mAh cm^{-2}) at a low electrolyte/sulfur ratio of less than 4 μL mg^{-1}. This positive feature implies the advanced electrochemical efficiency of our cathodes as compared to other high-loading cathodes at a lean electrolyte condition.[3-5,9]

Subsequently, we consider the cyclability of the high-loading sulfur cathodes at a lean electrolyte condition. In Figure 7c, we apply the suggested cycle life (200 cycles) and the required capacity retention (80%) for commercial lithium-sulfur cells as, respectively, the red and blue reference marks.[3,13-15] Clearly, our cathodes are the only case that keep a high electrochemical stability with a high amount of sulfur and a low amount of electrolyte in the cell. Our cathode also outperforms the benchmarks established for developing commercial lithium-sulfur cells with long cyclability.[3,13,14]

As a result, from Figures 7a to 7c, we assess the electrochemical performance of the state-of-the-art high-loading cathodes step-by-step from (1) high sulfur loading and content to (2) high effective capacity at a low electrolyte/sulfur ratio to (3) necessary cycle life and capacity retention. According to this analysis route, we demonstrate that our cathodes fulfill the multiple commercial requirements for designing and developing advanced lithium-sulfur cells with a high amount of sulfur, lean electrolyte, and long cycle life simultaneously.

CONCLUSION

A novel carbon-paper cathode substrate enables the design of a lithium-sulfur cell cathode that simultaneously allows the hosting of a high amount of sulfur with a lean electrolyte and displays enhanced cell performance with high electrochemical efficiency and stability. The

cathodes are able to host high sulfur loadings of 13 – 17 mg cm^{-2} with high sulfur contents of 75 – 80 wt.% and low electrolyte/sulfur ratios of 3.9 – 4.0 μL mg^{-1}. The improved cell characteristics result from the excellent electron/ion-transport capabilities of the cathode design—key factors for optimizing both the design parameters and cell performance of lithium-sulfur battery cathodes. Thus, even operating under such a strict cell-design condition, the cathodes demonstrate superior electrochemical efficiency with high gravimetric capacities of 535 and 473 mAh g^{-1}, areal capacities of 9.3 – 10.2 mAh cm^{-2}, and areal energy densities of 18.6 – 19.5 mWh cm^{-2}, as determined by taking into consideration the total mass of the cathode, including the carbon papers. The improved stability is reflected in the high capacity-retention rates of 71 – 85% after 200 cycles at a C/10 rate and good high-rate capability from C/20 to 1C rates. This work suggests that the application of conductive cathode substrates with limited nanoporosity could pave the way for the design and development of practical lithium-sulfur batteries that are competitive with the commercial lithium-ion cells.

METHODS

Carbon-paper cathode: Two layers of composited carbon fiber—carbon nanotube paper were used as the cathode substrate, in which polysulfide catholyte was injected and encapsulated to form the three-dimensional carbon-paper cathode. The carbon substrate (NanoTechLabs, Inc.) possessed a thickness of 70 μm, weight of 2.2 mg cm^{-2}, and a density of 300 mg cm^{-3}. Its microstructure showed an average pore size of 20 nm, a specific surface area of 80 m^2 g^{-1}, a total pore volume of 0.42 cm^3 g^{-1}, and no microporosity (see Figure S1 and Table S1 in the Supporting Information). The polysulfide catholyte contained 1.5 M Li_2S_6 dissolved polysulfides in a mixture of 1,3-dioxolane (99.8%, anhydrous, Sigma-Aldrich) and 1,2-dimethoxyethane

(99.5%, anhydrous, Sigma-Aldrich) (40 : 55 in vol : vol) with 1.85 M lithium bis(trifluoromethanesulfonyl)imide (99.95%, trace metal basis, Sigma-Aldrich) and 0.2 M lithium nitrate (99+%, extra pure, Acros Organics).[5,19,26] Additional blank electrolyte without Li_2S_6 polysulfides was used to wet a monolayer polypropylene separator with a thickness of 25 μm, pore size of 64 nm, and porosity of 55% (2500, Celgard). We formed the cell by placing the three-dimensional carbon-paper cathode containing 45 μL catholyte and 20 μL blank electrolyte on the separator for a sulfur loading of 13 mg cm^{-2}, sulfur content of 75 wt.%, and electrolyte/sulfur ratio of 4.0 μL mg^{-1}. We also formed another cell by placing a three-dimensional carbon-paper cathode containing 60 μL catholyte and 25 μL blank electrolyte on the separator for a sulfur loading of 17 mg cm^{-2}, sulfur content of 80 wt.%, and electrolyte/sulfur ratio of 3.9 μL mg^{-1}. No additional binders or aluminum-foil current collectors were used in the cathode, making the effective, practical capacity high.

Material Characterization: Microstructure and porosity were analyzed based on nitrogen adsorption-desorption isotherms that were measured at 77 K with an automated gas sorption analyzer (AutoSorb iQ2, Quantachrome Instruments). The specific surface area, pore-size distribution, and total pore volume were calculated with, respectively, the Brunauer-Emmett-Teller, Barrett-Joyner-Halenda, and T-plot analysis.[3,5,26] The morphology of the cells was determined using a field-emission scanning electron microscope (FE-SEM; Quanta 650, FEI). Elemental mapping, elemental intensity spectra, and line analysis were collected by an energy dispersive x-ray spectroscopy detector (EDS; Bruker system). The freshly-made cathodes and the fully-cycled cathodes were retrieved, respectively, from newly-assembled cells after sealing and resting the materials for 30 min and from the cycled cells after 200 cycles. Both the freshly-made

cathodes and cycled cathodes were stored in a sealed argon-filled vessel and delivered for microstructural and elemental analyses within 30 min. Surface electrical resistivity was measured with a four-point-probe head (SP4, Lucas Labs) and a source meter (Model 2400 general-purpose source meter, Keithley) by the four-wire sense-mode resistivity measurement (Pro4, Lucas Labs).

Performance Characterization: Electrochemical testing was carried out with standard CR2032 coin cells using a nickel-foam spacer (Pred Materials), lithium-metal counter electrodes (99.9%, trace metal basis, Sigma-Aldrich), wetted separators, and cathodes (sulfur mass: 13 and 17 mg per cathode).[3,5,30] Pouch cells were assembled with lithium-metal counter electrodes, wetted separators, and cathodes (sulfur mass: 51.9 mg per cathode) in a transparent zipbag. All as-prepared cells were charged to 3.0 V and subsequently applied for various electrochemical analyses. Electrochemical utilization, cycle stability, and voltage profiles were collected with a programmable battery cycler (Arbin) by discharging the cells to 1.6 V and then charging to 2.7 V for a full cycle at C/10, C/7, and C/5 rates. Pouch cells were operated at 1.5 – 3.0 V. Long-term cyclability was analyzed at a C/10 rate for 200 cycles and high-rate capability was demonstrated from C/20 to 1C rates three times during a 210 cycle analysis. Specifically, we set the cycling rate at C/20 for 1 – 10, 71 – 80, and 141 – 150 cycles, at C/10 for 11 – 20, 81 – 90, and 151 – 160 cycles, at C/7 for 21 – 30, 91 – 100, and 161 – 170 cycles, at C/5 for 31 – 40, 101 – 110, and 171 – 180 cycles, at C/3 for 41– 50, 111 – 120, and 181– 190 cycles, at C/2 for 51 – 60, 121 – 130, and 191 – 200 cycles, and at 1C for 61– 70, 131 – 140, and 201 – 210 cycles.

Electrochemical Analysis: EIS results were obtained with a potentiostat (SI 1287, Solartron) as the electrochemical interface coupled with an impedance analyzer (SI 1260, Solartron). The data was recorded by Zplot in the frequency range of 1 MHz to 100 mHz with an AC voltage amplitude of 5 mV and analyzed by Zivew for the simulation and fitting interface. CV measurements were evaluated with a universal potentiostat (VoltaLab PGZ 402, Radiometer Analytical) in the voltage window of 1.6 – 2.7 V at a scan rate of 0.02, 0.03, and 0.04 mV s^{-1}. In order to normalize the analytical data for the EIS and CV analyses, the cells were selected by a narrow open-circuit voltage range of 2.29 V with standard deviations (SD) of 0.029 and 0.0076 for the cathodes with sulfur loadings of, respectively, 13 and 17 mg cm^{-2}. The lithium-ion diffusion coefficient was calculated by the Randles-Sevick equation: $I = 268{,}600 \times N_{(electron)}^{1.5} \times A \times D_{(lithium)}^{0.5} \times V^{0.5} \times C_{(lithium)}$, in which V is the scanning rate (V s^{-1}) applied in CV, I indicates the resulting peak current (A) of the cathodic (C1, C2) and anodic peaks (A1, A2), $N_{(electron)}$ is the number of electrons involved in the reaction, A is the electrode area (cm^2), and $D_{(lithium)}$ and $C_{(lithium)}$ are the lithium-ion diffusion coefficient (cm^2 s^{-1}) and the lithium-ion concentration in the electrolyte (mol mL^{-1}), respectively.[31-33]

FIGURES

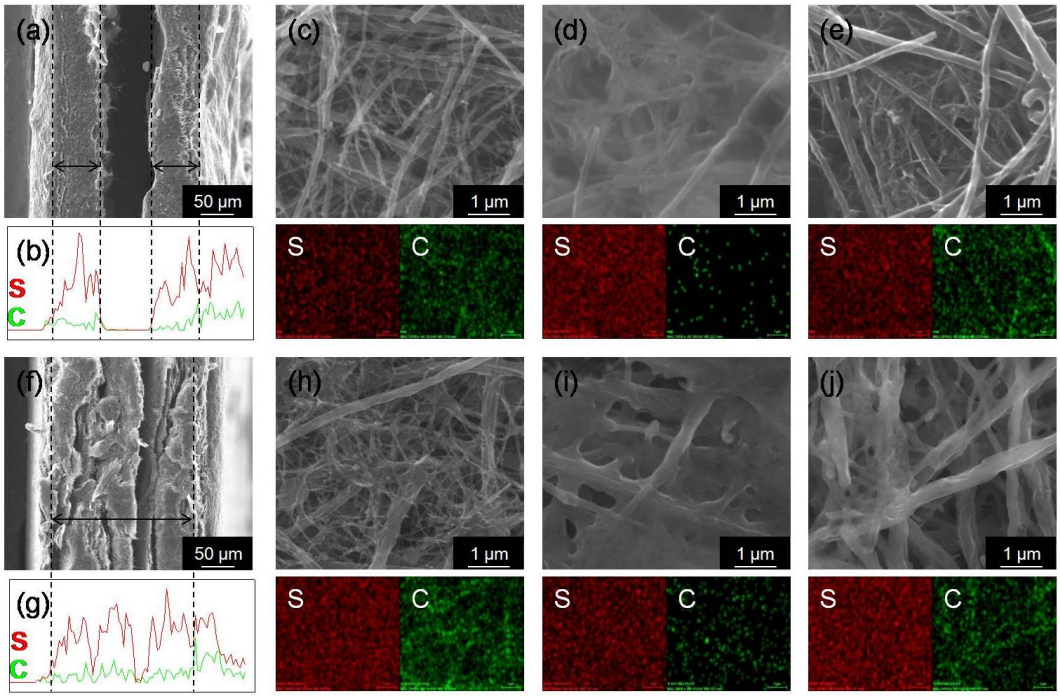

Figure 1. Morphology and microstructure of the cathode. (a) Cross-sectional SEM, (b) EDS line scan, (c) aerial-view SEM/EDS of the top surface, (d) aerial-view SEM/EDS inspection from the inside surface after opening the cathode, and (e) aerial-view SEM/EDS inspection of the bottom surface of a freshly-made cathode. (f) Cross-sectional SEM, (g) EDS line scan, (h) aerial-view SEM/EDS of the top surface, (i) aerial-view SEM/EDS of the inside surface after opening the cathode, and (j) aerial-view SEM/EDS of the bottom surface of a cycled cathode after 200 cycles.

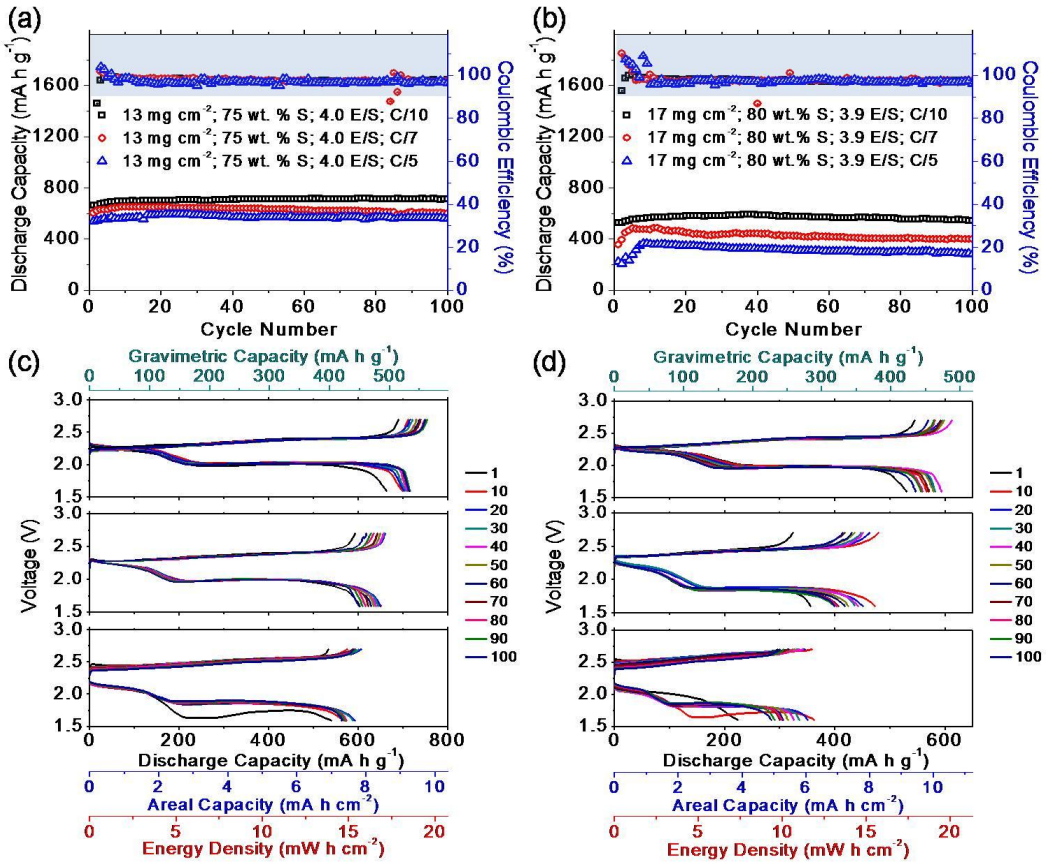

Figure 2. Electrochemical performance. (a,b) Cyclability and (c,d) voltage profiles of the three-dimensional carbon-paper cathode. In a and c, the cells have sulfur loading and content values of 13 mg cm^{-2} and 75 wt.%, respectively, and an electrolyte/sulfur ratio of 4.0 µL mg^{-1}. In b and d, the cells have sulfur loading and content values of 17 mg cm^{-2} and 80 wt.%, respectively, with an electrolyte/sulfur ratio of 3.9 µL mg^{-1}.

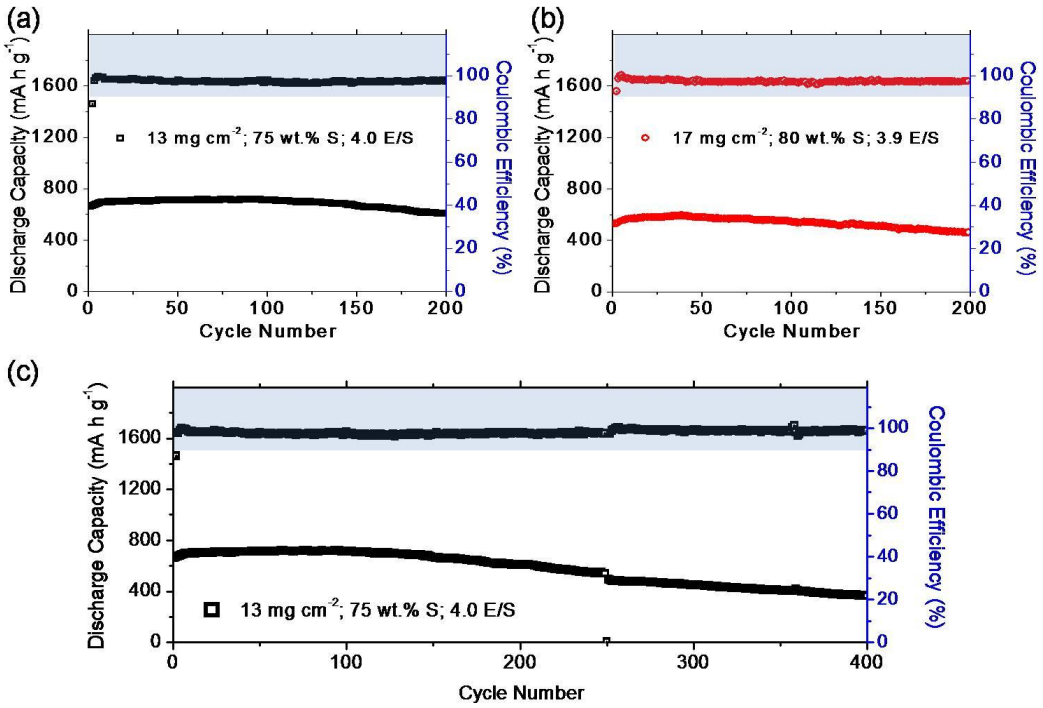

Figure 3. Long-term cyclability of the cells fabricated with the three-dimensional carbon-paper cathodes with sulfur loading and sulfur content values of (a) 13 mg cm^{-2} and 75 wt.%, respectively, with an electrolyte/sulfur ratio of 4.0 μL mg^{-1} and (b) 17 mg cm^{-2} and 80 wt.%, respectively, with an electrolyte/sulfur ratio of 3.9 μL mg^{-1}. (c) Extended cycle testing of a.

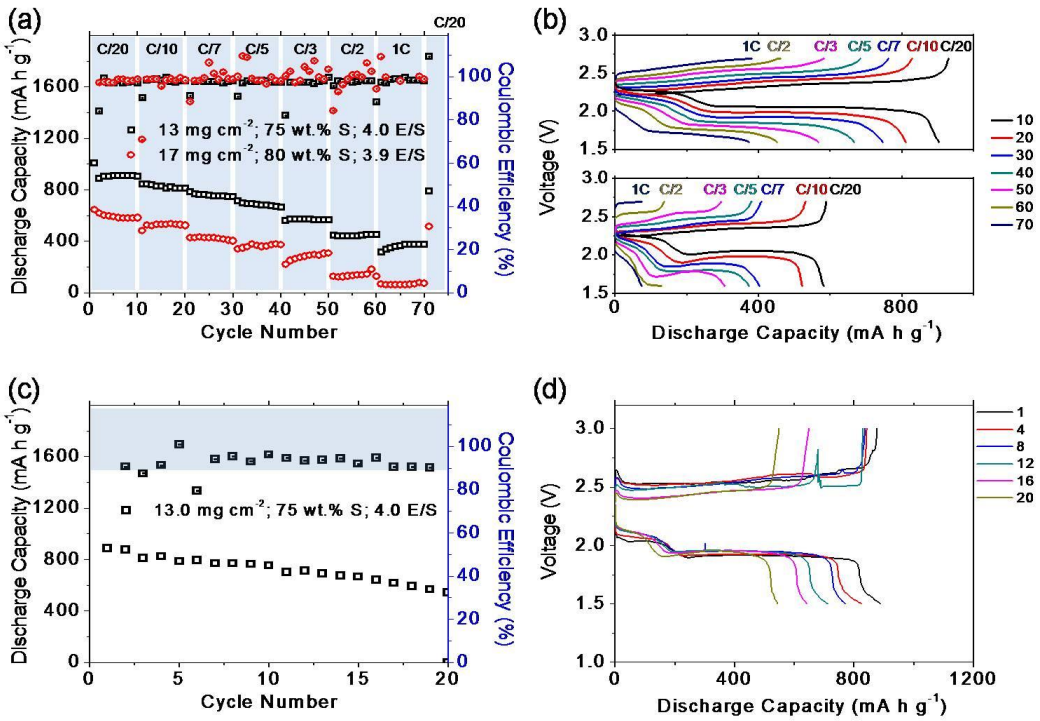

Figure 4. Electrochemical testing. (a) High-rate capability of the cells fabricated with the three-dimensional carbon-paper cathodes with lean electrolyte. (b) Voltage profiles of a. (c) Cyclability of a transparent pouch cell. (d) Voltage profiles of c.

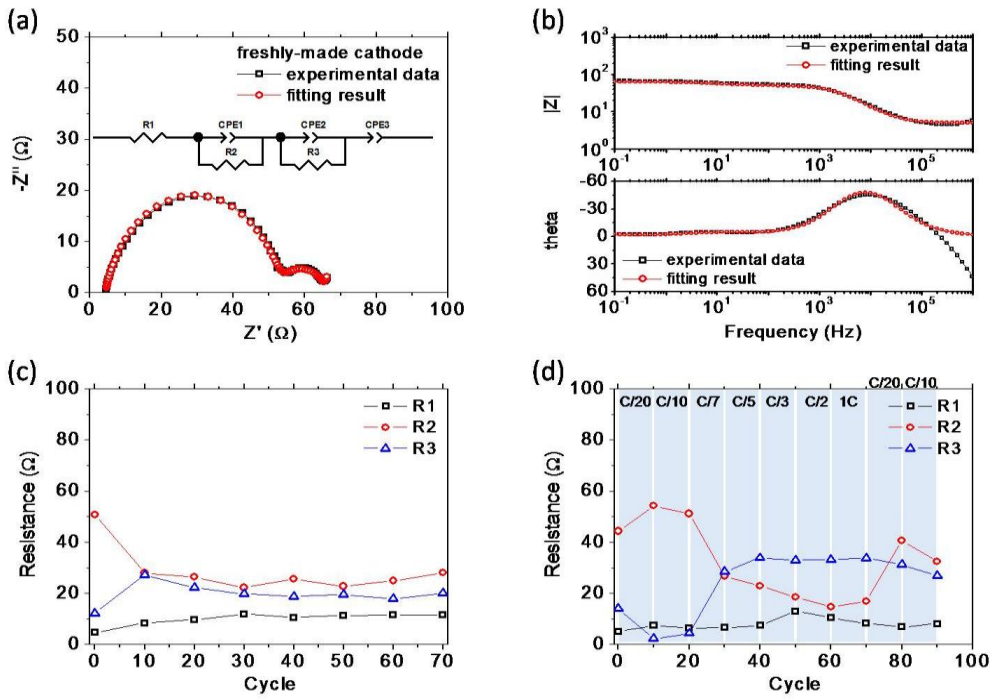

Figure 5. Electrochemical impedance measurements. (a) Nyquist plots. (b) Bode plots. (c) Resistance as a function of cycle number. (d) Resistance as a function of cycle rate. The impedance data were collected from the cells fabricated with the three-dimensional carbon-paper cathodes with sulfur loading and sulfur content values of 13 mg cm^{-2} and 75 wt.%, respectively, with an electrolyte/sulfur ratio of 4.0 μL mg^{-1}. The resistance shown in c and d are the electrolyte and the internal ohmic resistance of the cell referred as R1, the interfacial contact resistance as R2, and the charge-transfer resistance as R3.

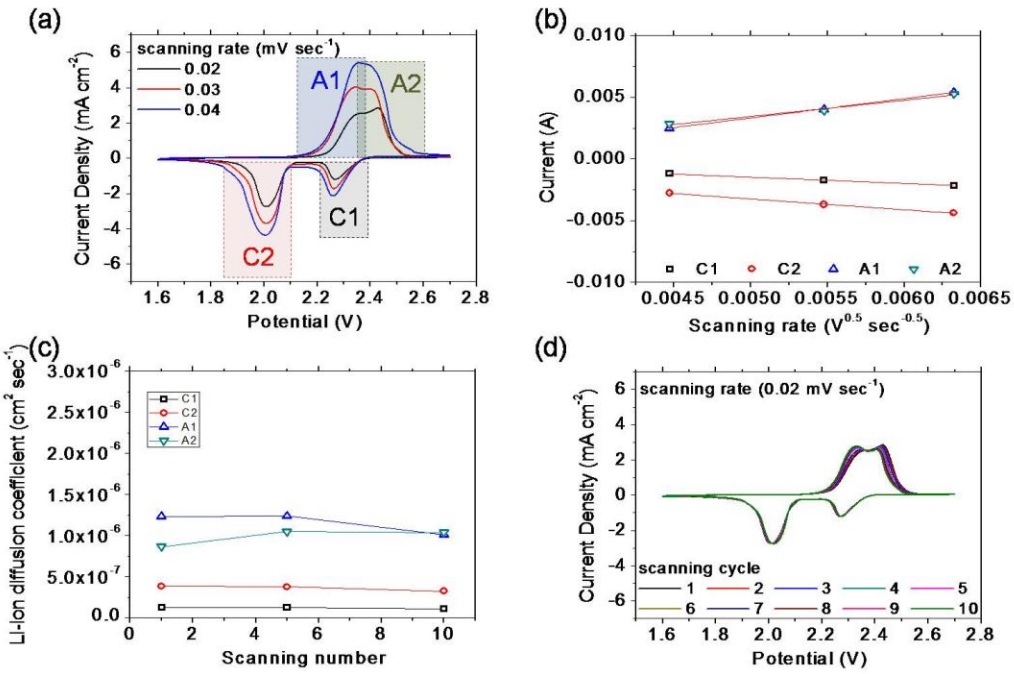

Figure 6. Electrochemical reversibility characteristics of the cells fabricated with the three-dimensional carbon-paper cathodes with lean electrolyte . (a) CV plots. (b) Linear fitting of peak current and $V^{0.5}$ of a. (c) Li-ion diffusion coefficient. (d) Reversible CV scanning.

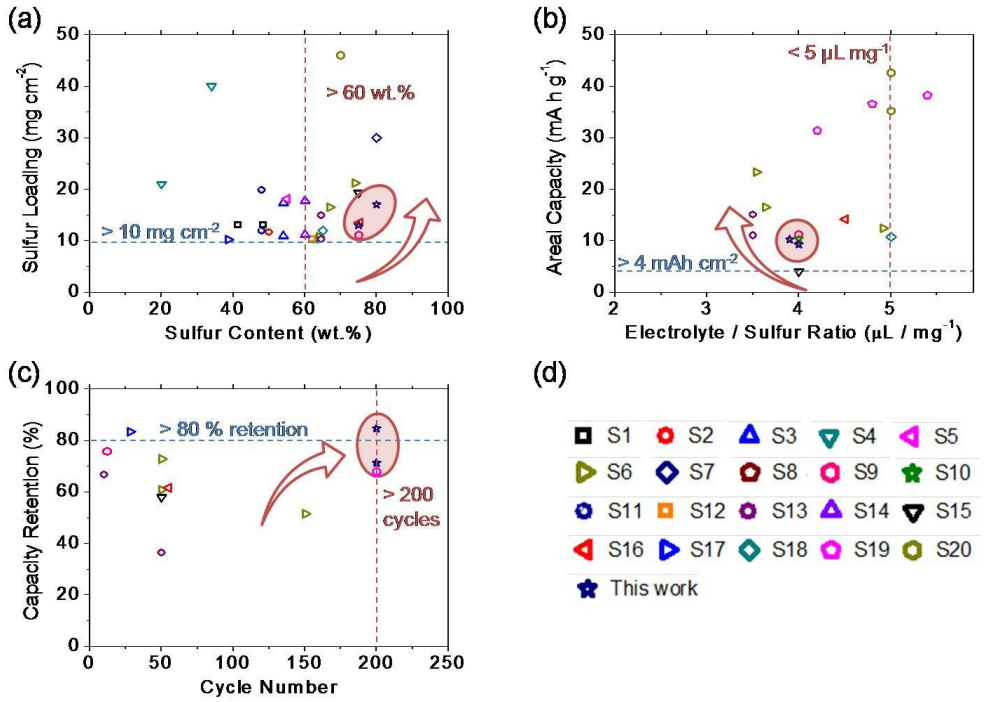

Figure 7. Performances on the state-of-the-art lithium-sulfur battery cathodes in a step-by-step consideration of various conditions: (a) sulfur loading and sulfur content, (b) effective capacity at a low electrolyte/sulfur ratio, and (c) cycle life and capacity retention. The red arrows direct the development tendency. (d.) List of reference articles (see Table S2, references S1 – S20, in the supporting information).

ASSOCIATED CONTENT

Corresponding Author

*E-mail: manth@austin.utexas.edu

Author Contributions

The manuscript was written through contributions of all authors. All authors have given approval to the final version of the manuscript.

Acknowledgment

This work was supported by the Department of Energy, Office of Energy Efficiency and Renewable Energy (EERE), under Award Number DE-EE0007218.

Supporting Information

Supporting Information Available: Analyses of physiochemical characteristics, microstructure, element, cell characteristics, rate performance, pouch cells, impedance, and cyclic voltammetry. This material is available free of charge *via* the Internet at http://pubs.acs.org.

REFERENCES

1. Manthiram, A.; Chung, S.-H.; Zu, C. Lithium–Sulfur Batteries: Progress and Prospects. *Adv. Mater.* **2015**, *27*, 1980-2006.
2. Yin, Y.-X.; Xin, S.; Guo, Y.-G.; Wan, L.-J. Lithium–Sulfur Batteries: Electrochemistry, Materials, and Prospects. *Angew. Chem. Int. Ed.* **2013**, *52*, 13186-13200.
3. Chung, S.-H.; Chang, C.-H.; Manthiram, A. Progress on the Critical Parameters for Lithium–Sulfur Batteries to be Practically Viable. *Adv. Funct. Mater.* **2018**, *28*, 1801188.
4. Li, M.; Lu, J.; Chen, Z.; Amine, K. 30 Years of Lithium- Ion Batteries. *Adv. Mater.* **2018**, *30*, 1800561.
5. Chung, S.-H.; Manthiram, A. Designing Lithium-Sulfur Cells with Practically Necessary Parameters. *Joule* **2018**, *2*, 710-724.
6. Eroglu, D.; Zavadil, K. R.; Gallagher, K. G. Critical Link between Materials Chemistry and Cell-Level Design for High Energy Density and Low Cost Lithium–Sulfur Transportation Battery. *J. Electrochem. Soc.* **2015**, *162*, A982-A990.
7. Hagen, M.; Hanselmann, D.; Ahlbrecht, K.; Maça, R.; Gerber, D.; Tübke, J. Lithium–Sulfur Cells: The Gap between the State-of-the-Art and the Requirements for High Energy Battery Cells. *Adv. Energy Mater.* **2015**, *5*, 1401986.
8. Gao, J.; Abruña, H. D. Key Parameters Governing the Energy Density of Rechargeable Li/S Batteries. *J. Phys. Chem. Lett.* **2014**, *5*, 882-885.
9. Fang, R.; Zhao, S.; Sun, Z.; Wang, D.-W.; Cheng, H.-M.; Li, F. More Reliable Lithium- Sulfur Batteries: Status, Solutions and Prospects. *Adv. Mater.* **2017**, *29*, 1606823.

10. McCloskey, B. D. Attainable Gravimetric and Volumetric Energy Density of Li–S and Li Ion Battery Cells with Solid Separator-Protected Li Metal Anodes. *J. Phys. Chem. Lett.* **2015**, *6*, 4581-4588.

11. Peng, H.-J.; Huang, J.-Q.; Cheng, X.-B.; Zhang, Q. Lithium- Sulfur Batteries: Review on High- Loading and High- Energy Lithium–Sulfur Batteries. *Adv. Energy Mater.* **2017**, *7*, 1700260.

12. Hagen, M.; Fanz, P.; Tübke, J. Cell Energy Density and Electrolyte/Sulfur Ratio in Li–S Cells. *J. Power Sources* **2014**, *264*, 30-34.

13. Cleaver, T.; Kovacik, P.; Marinescu, M.; Zhang, T.; Offer, G. Perspective—Commercializing Lithium Sulfur Batteries: Are We Doing the Right Research? *J. Electrochem. Soc.* **2018**, *165*, A6029-A6033.

14. Cell Specification, Oxis Energy, High gravimetric energy density, Rechargeable Li-S Pouch Cell, https://45uevg34gwlltnbsf2plyua1-wpengine.netdna-ssl.com/wp-content/uploads/2018/05/OXIS-Li-S-Ultra-Light-Cell-v4.05.pdf, accessed: 05, 2018.

15. Zhang, T.; Marinescu, M.; Walus, S.; Kovacik, P.; Offer, G. J. What Limits the Rate Capability of Li-S Batteries during Discharge: Charge Transfer or Mass Transfer? *J. Electrochem. Soc.* **2018**, *165*, A6001-A6004.

16. Li, S.-Y.; Wang, W.-P.; Duan, H.; Guo, Y.-G. Recent progress on confinement of polysulfides through physical and chemical methods. *J. Energy Chem.* **2018**, *27*, 1555-A6004..

17. Lu. D.; Zheng, J.; Li, Q.; Xie, X.; Ferrara, S.; Nie, Z.; Mehdi, L. B.; Browning, N. D.; Zhang, J.-G.; Graff, G. L.; Liu, J.; Xiao, J. High Energy Density Lithium–Sulfur Batteries: Challenges of Thick Sulfur Cathodes. *Adv. Energy Mater.* **2015**, *5*, 1402290.

18. Chung, S.-H.; Chang, C.-H.; Manthiram, A. A Core–Shell Electrode for Dynamically and Statically Stable Li–S Battery Chemistry. *Energy Environ. Sci.* **2016**, *9*, 3188-3200.

19. Mikhaylik, Y. V.; Akridge, J. R. Polysulfide Shuttle Study in the Li/S Battery System. *J. Electrochem. Soc.* **2004**, *151*, A1969-A1976.

20. Chen, J.; Henderson, W. A.; Pan, H.; Perdue, B. R.; Cao, R.; Hu, J. Z.; Wan, C.; Han, K. S.; Muller, K. T.; Zhang, J.-G.; Shao, Y.; Liu, J. Improving Lithium–Sulfur Battery Performance under Lean Electrolyte through Nanoscale Confinement in Soft Swellable Gels. *Nano Lett.* **2017**, *17*, 3061-3067.

21. Chen, S.; Gao, Y.; Yu, Z.; Gordin, M. L.; Song, J.; Wang, D. High Capacity of Lithium-Sulfur Batteries at Low Electrolyte/Sulfur Ratio Enabled by an Organosulfide Containing Electrolyte. *Nano Energy* **2017**, *31*, 418-423.

22. Chung, S.-H.; Manthiram, A. Lithium–Sulfur Batteries with Superior Cycle Stability by Employing Porous Current Collectors. *Electrochim. Acta* **2013**, *107*, 569-576.

23. Fang, R.; Zhao, S.; Pei, S.; Qian, X.; Hou, P.-X.; Cheng, H.-M.; Liu, C.; Li, F. Toward More Reliable Lithium–Sulfur Batteries: An All-Graphene Cathode Structure. *ACS Nano* **2016**, *10*, 8676-8682.

24. Huang, J.-Q.; Zhang, Q.; Wei, F. Multi–Functional Separator/Interlayer System for High–Stable Lithium–Sulfur Batteries: Progress and Prospect. *Energy Storage Mater.* **2015**, *1*, 127-145.

25. Wu. M.; Cui, Y.; Bhargav, A.; Losovyj, Y.; Siegel, A.; Agarwal, M.; Ma, Y.; Fu, Y. Organotrisulfide: A High Capacity Cathode Material for Rechargeable Lithium Batteries. *Angew. Chem. Int. Ed.* **2016**, *55*, 10027-10031.

26. Chung, S.-H.; Manthiram, A. Rational Design of Statically and Dynamically Stable Lithium–Sulfur Batteries with High Sulfur Loading and Low Electrolyte/Sulfur Ratio. *Adv. Mater.* **2018**, *30*, 1705951.

27. Xiao, J. Understanding the Lithium Sulfur Battery System at Relevant Scales. *Adv. Energy Mater.* **2015**, *5*, 1501102.

28. Pope, M. A.; Aksay, I. A. Structural Design of Cathodes for Li–S Batteries. *Adv. Energy Mater.* **2015**, *5*, 1500124.

29. Yang, J.; Xie, J.; Zhou, X.; Zou, Y.; Tang, J.; Wang, S.; Chen, F.; Wang, L. Functionalized N- Doped Porous Carbon Nanofiber Webs for a Lithium−Sulfur Battery with High Capacity and Rate Performance. *J. Phys. Chem. C* **2014**, *118*, 1800-1807.

30. Kim, M. S.; Ma, L.; Choudhury, S.; Archer. L. A. Multifunctional Separator Coatings for High- Performance Lithium–Sulfur Batteries. *Adv. Mater. Interface* **2016**, *3*, 1600450.

31. Zhang, G.; Zhang, Z.-W.; Peng, H.-J.; Huang, J.-Q.; Zhang, Q. Lithium–Sulfur Batteries: A Toolbox for Lithium–Sulfur Battery Research: Methods and Protocols. *Small Methods* **2017**, *1*, 1700134.

32. Chung, S.-H.; Chang, C.-H.; Manthiram, A. A Carbon-Cotton Cathode with Ultrahigh-Loading Capability for Statically and Dynamically Stable Lithium–Sulfur Batteries. *ACS Nano* **2016**, *10*, 10462-10470.

33. Luo, L.; Chung, S.-H.; Manthiram, A. Rational Design of a Dual- Function Hybrid Cathode Substrate for Lithium–Sulfur Batteries. *Adv. Energy Mater.* **2018**, *8*, 1801014.

34. Kazazi, M.; Vaezi, M. R.; Kazemzadeh, A. Enhanced Rate Performance of Polypyrrole-Coated Sulfur/MWCNT Cathode Material: A Kinetic Study by Electrochemical Impedance Spectroscopy. *Ionics* **2014**, *20*, 635-643.

35. Lochala, J.; Liu, D.; We, B.; Robinson, C.; Xiao, J. Research Progress toward the Practical Applications of Lithium–Sulfur Batteries. *ACS Appl. Mater. Interfaces* **2017**, *9*, 24407-24421.

36. Xu, W.; Wang, J.; Ding, F.; Chen, X.; Nasybulin, E.; Zhang, Y.; Zhang, J.-G. Lithium Metal Anodes for Rechargeable Batteries. *Energy Environ. Sci.* **2014**, *7*, 513-537.

37. Wang, J.; Lin, F.; Jia, H.; Yang, J.; Monroe, C. W.; NuLi, Y. Towards a Safe Lithium-Sulfur Battery with a Flame-Inhibiting Electrolyte and a Sulfur-Based Composite Cathode. *Angew. Chem. Int. Ed*. **2014**, *53*, 10099-10104.

38. Deng, Z.; Zhang, Z.; Lai, Y.; Liu, J.; Li, J.; Liu, Y. Electrochemical Impedance Spectroscopy Study of a Lithium/Sulfur Battery: Modeling and Analysis of Capacity Fading. *J. Electrochem. Soc.* **2013**, *164*, A553-A558.

39. Zhang, J.; Li, J.-Y.; Wang, W.-P.; Zhang, X.-H.; Tan, X.-H.; Chu, W.-G.; Guo, Y.-G. Microemulsion Assisted Assembly of 3D Porous S/Graphene@g- C_3N_4 Hybrid Sponge as Free- Standing Cathodes for High Energy Density Li–S Batteries. *Adv. Energy Mater.* **2018**, *8*, 1702839.

40. Chen, X.; Hou, T.; Persson, K. A.; Zhang, Q. Combining Theory and Experiment in Lithium–Sulfur Batteries: Current Progress and Future Perspectives. *Mat. Today*, DOI: 10.1016/j.mattod.2018.04.007.

Table of Contents Graphic and Synopsis